Structural Health Monitoring for Bell 407 Tail Boom

Ashish Purekar, Kunal Kothari
Techno-Sciences, Inc.
Beltsville, Maryland

Young-Tai Choi*, Norman M. Wereley[†]
*Assistant Research Scientist, [†]Professor – Aerospace Engineering
University of Maryland
College Park, Maryland

Henry Wilson
Chief, Research Structures and Internal Loads Engineering
Bell Helicopters Textron Inc.
Ft. Worth, Texas

Nathaniel Bordick
Aviation Applied Technology Directorate
Ft. Eustis, VA

Abstract

Structural Health Monitoring (SHM) of aerospace structures has received significant interest as a core component of Condition Based Maintenance (CBM). An Acousto-Ultrasonic method based on high frequency structural vibrations using piezoelectric transducers has been developed to perform damage detection on metallic and composite aerospace structures. Tests were performed on laboratory specimens to evaluate the sensitivity of crack detection and ballistic damage using this method. The Bell 407 tail boom structure was chosen to demonstrate the capability a system, designed to employ the developed method, to detect common structural damage related to fatigue cracking and battle damage.

Introduction

The aerospace community has been investigating Structural Health Monitoring (SHM) techniques for various platforms ([1], [2], [3], [4], [5]). SHM techniques are part of an overall Condition Based Maintenance (CBM) system aimed to reduce maintenance requirements by providing a diagnostic and prognostic capability. Resources saved due to a reduction in maintenance and parts replacement reduces the total operating and sustainment costs of the platform. When extended across a military or civilian fleet of aircraft, the cost savings becomes significant.

Helicopters are attractive platforms for application of SHM technologies [6] due to the environment in which they operate where severe vibration loads and varying mission profiles can induce damage in the structure. The Bell 407 tail boom, pictured in Figure 1, was chosen as the specific Primary Structural Element (PSE) to demonstrate in-situ SHM technologies due to fatigue and ballistic related damage. While the Bell 407 is a civilian system, it is similar in design to the US Army OH-58 Kiowa. The structural health monitoring technologies can, however, be transitioned to any military or civilian platform.

Figure 1: Bell 407

High frequency wave propagation has been investigated for damage detection in structures ([7], [8], [9], [10], [11]). Common methods include Acousto-Ultrasonics and Guided Waves. These methods have shown the ability to detect damage in structural components. Transduction can be provided using a wide number of devices. Commonly, active materials are used to excite and sense high frequency wave propagation in structures. The active materials are typically of a small profile and low-weight which make them well suited for application to aerospace systems.

For thin panel structures, wave propagation is described using Lamb wave modes. The two basic modes are A0 and S0, which are equivalent to low speed bending and in-plane modes, respectively. The propagation of these modes in structures, in addition to interactions with boundaries and damage, has been investigated for damage detection purposes on flat metallic and composite panels. The damage detection

portion of this study focuses on fatigue crack and ballistic damage; however could also be used to detect material loss associated with corrosion.

System Description

A Structural Health Monitoring (SHM) system tailored for an aerospace application is subject to restrictions due to the operational environment. The hardware components of an SHM system must be reliable, durable, have a low profile and small footprint, and add as little weight as possible.

Hardware components of this SHM system consist of mounted transducers, data acquisition, and processing units. A diagram of a conceptual transducer network for SHM is shown in Figure 2. Transducers are mounted to structural components of interest and designed to evaluate damage conditions. A link to a ground station unit enables data archiving and implementation of fleet-wide health monitoring and maintenance coordination.

The implementation of such a system depends on a number of system level parameters including overall weight, suitability for in-flight operation, and scheduling requirements. For in-flight operation, all of the hardware components would be mounted on the platform. In the case of on-ground SHM activities, only the transducers would be mounted to the structural components, data acquisition and processing facilities would interface with the transducers on the ground.
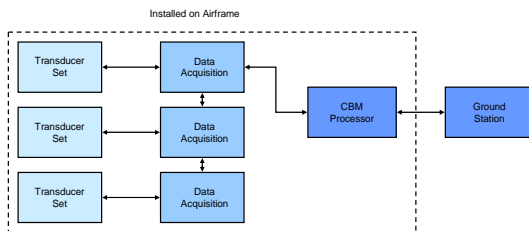

Figure 2: Transducer network configuration

The transducers used for structural health monitoring consist of piezoelectric elements which are used as sensors or actuators depending on the specific purpose. The piezoelectric elements are 0.25 in diameter and 0.0075 in. thick with an overall weight of approximately 0.2 grams. A number of transducer elements may be mounted without adding significant weight. The data acquisition unit is specifically designed for the piezoelectric transducer elements and tailored toward the acquisition requirements of the Acousto-Ultrasonic method of damage detection. Health and Usage Monitoring System (HUMS) units on the platform consolidate information from a variety of sensors and systems to determine maintenance actions. The HUMS processor runs the diagnostic routines on the signals provided by the data acquisition unit. Since the HUMS processor handles the computation work, the data acquisition unit can be designed as a small device.

Application to Helicopter Airframe

Fatigue damage is caused by stress concentrations and cyclic loads. While there are several fatigue sensitive locations on the aircraft, the Bell 407 tail boom structure was chosen to demonstrate the sensor technology. The two main areas of interest for damage detection on the Bell 407 tail boom are identified as the inter-costal members used to mount the tail boom to the airframe and the area around the horizontal stabilizer, both circled in Figure 3. Vibratory loads from the helicopter downwash and tail rotor vibrations induce stresses around the cut-out for the horizontal stabilizer. Stress concentrations in these regions lead to fatigue cracking between rivets at the interface of the horizontal stabilizer and the tail boom.
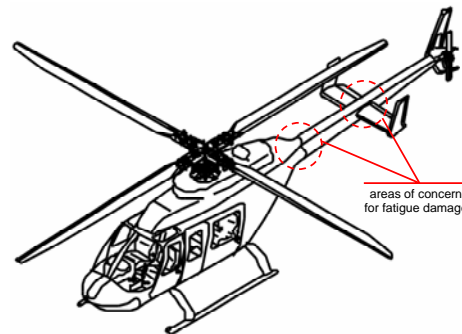

Figure 3: Fatigue hot spots on Bell 407

The Bell 407 tail boom will also be used to demonstrate battle damage detection capability. Monitoring for impact and ballistic damage in both the skin and underlying support structure is an integral part of a SHM system for military platforms.

Wave Propagation in Tail Boom Section

The Bell 407 tail boom consists of metallic monocoque construction with frame section distributed along the length. A section of the tail boom was instrumented using piezoelectric transducers to excite and sense high frequency structural waves. The transducers were made of PZT-5A materials and were approximately 0.125 in. in diameter and 0.0075 in thickness. A picture of the test section with mounted transducers is shown in Figure 4. Each transducer can

be used as an actuator or sensor; however for this specific case the transducer at the end of the section was used as the excitation element and the remaining transducers were used as sensor elements. There was a distance of approximately 6 in. between each transducer.
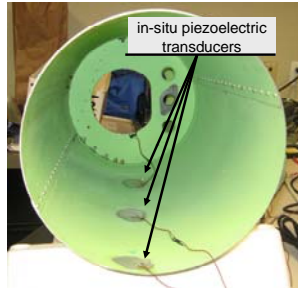

Figure 4: In-situ transducers mounted in Bell 407 tailboom

High frequency tone burst signals from 40 kHz to 200 kHz were introduced into the structure by the excitation element and the sensors were used to monitor the passage of the A0 Lamb waves as they propagated outward. The transient sensor response was gathered at each test frequency. A plot of the transient response from 100 kHz excitation is shown in Figure 5. The initial response shows EMI noise followed by the passage of the A0 Lamb mode as it travels down the tail boom through each of the sensors. Subsequent waveforms correspond to reflections from boundaries and edges in the test section. The group speed was determined at each of the test frequencies and compared to models of wave propagation for thin flat panels. The Kirchoff bending mode [12], based on a simplified model of a thin panel, does not allow for shear deformation through the thickness. The A0 Lamb model is based on a higher order theory [13]. The comparison between the theories and experimental results are shown in Figure 6. The results show the two models start diverging as the frequency increases above 50 kHz excitation. Additionally, the A0 Lamb mode model follows experimental trends more closely than the Kirchoff model. The model produces group speed predictions approximately 10% higher than experimentally observed. This could be due small differences in materials properties, skin thickness, and sensor placement.

This test confirmed the feasibility of using high frequency wave propagation and in-situ piezoelectric sensors for active interrogation of the tail boom structure.
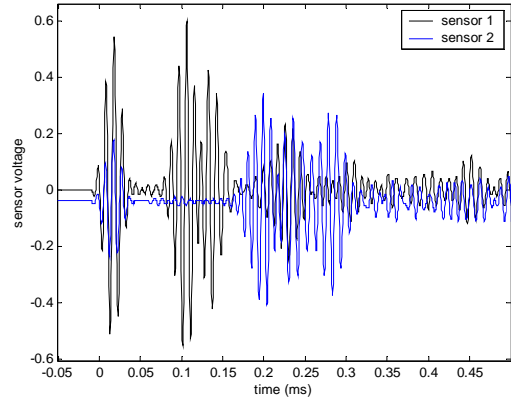

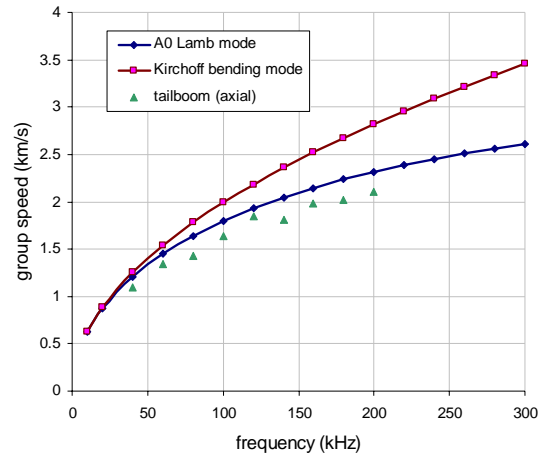Figure 5: Transient response at 100 kHz excitation

Figure 6: Comparison between theory and experiment

Fatigue Damage

The area of the Bell 407 tail boom most prone to fatigue damage is directly fore and aft of the horizontal stabilizer. History has shown crack initiation at the fastener positions shown in Figure 7.
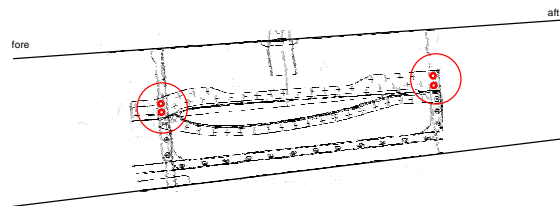

Figure 7: Fatigue cracking hot spots

Coupon level testing was conducted to determine if the wave based approach was capable of detecting fatigue damage comparable to what has been seen in the tail boom. A coupon specimen, representing the tail boom hot spot, was constructed out of 0.04 in thick Aluminum 2024-T3. The coupon was 0.8 in. wide and

24 in. long. A diagram of the coupon specimen is shown in Figure 8. A chevron notch that had a depth of approximately 0.164 in. and a span of 0.05 in. was cut into the coupon. Mechanical loading was applied using a MTS test frame with tension-tension loading from 100 MPa to 195 MPa at 1 Hz frequency. One piezoelectric transducer was used as an actuator and five transducers were placed between the actuator element and the notch. Each transducer was a 0.25 in. diameter PZT-5A piezoceramic element. Data was acquired every 600-800 cycles after crack initiation was observed. Data was acquired for two cases, (1) a crack open case where a tensile load of approximately 100 lbs was used and (2) a crack closed case where the bottom grip on the MTS machine was released.

(a) diagram   (b) coupon in load frame
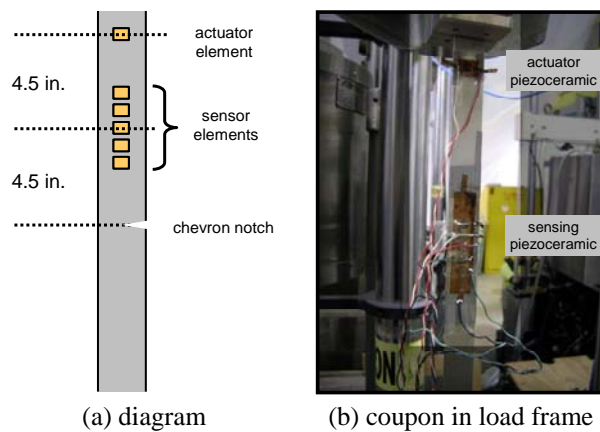
Figure 8: Coupon specimen for fatigue crack detection

Fatigue testing of the coupon specimen produced stable crack growth up to a length of approximately 0.2 in. The curve in Figure 9 shows the growth in the crack with the number of cycles. The set of images in Figure 10 show the growth in the crack as the number of cycles increased. After a 0.20 in. crack depth was observed and subsequently loaded, the specimen critically failed.
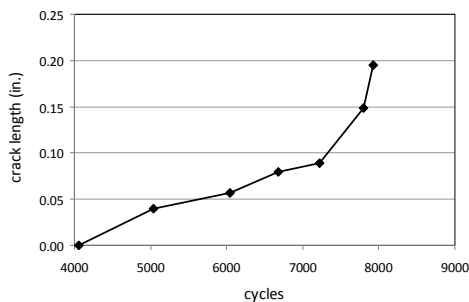

Figure 9: Growth of crack with loading cycles

(a) chevron notch

(b) 0.057 in. crack length   (c) 0.08 in crack length
(6k cycles)   (7.2k cycles)

(d) 0.15 in. crack length   (d) 0.20 in. crack length
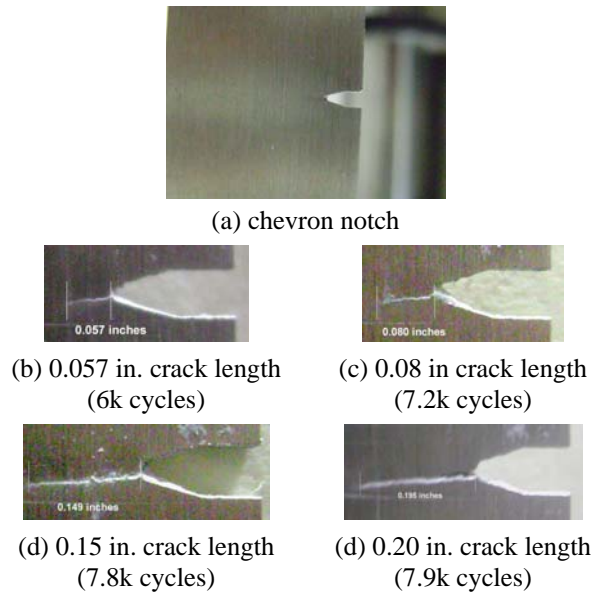(7.8k cycles)   (7.9k cycles)

Figure 10: Crack propagation in coupon specimen

The actuator transducer was excited using a 5 cycle tone burst of 60 kHz, 80 kHz, and 100 kHz. The transient data was captured by the sensor elements. The transient time histories were windowed based on the expected flight time of the interrogating signal from the actuator to the notch and back to the center of the sensor. The transient data was captured and signal processing algorithms were used to compare the signals in the undamaged and baseline cases. The data reduction step produced damage indices, which are used as a diagnostic metric. Damage indices were computed based on the time domain response and averaged across all sensor elements and frequencies. The damage indices are plotted for both the crack open and crack closed cases (Figure 11). In both cases, the damage index is shown to rise as the crack length increases. The damage index levels for the open crack were higher than the closed crack cases. The test results showed that the guided wave damage detection technique is capable of detecting and tracking fatigue crack growth.
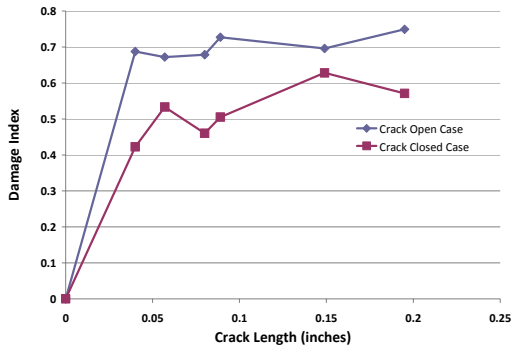
Figure 11: Monitoring of crack growth

The proposed transducer layout is shown in Figure 12 for the regions to the fore and aft of the horizontal stabilizer. This arrangement enables monitoring of the two hot spot regions in the tail boom section prone to fatigue damage.
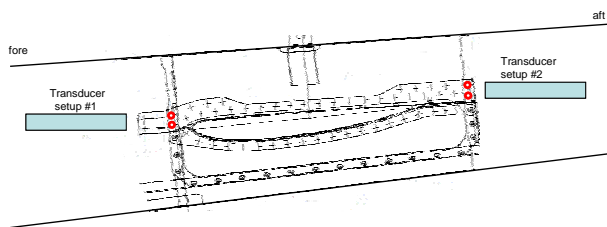

Figure 12: Transducer layout for fatigue monitoring

Detection of Ballistic Battle Damage - Skin

Detection of ballistic battle damage can be performed by either using an active or passive approach. In the passive approach, sensors continuously monitoring the structure for a singular incident related to impact. The location and severity of the ballistic damage is determined based on the transient response of the structure due to the impact. The sensor signals are compared to analytical or empirical formulations of the transient response of the structure. For a simple panel structure with a small number of sensors, this type of approach is practical; however, the difficulty of the passive approach significantly increases with structural complexity. Modeling the high frequency transient response of a tail boom type structure would be extremely complicated. Additionally, if multiple structural configurations are to be monitored, the data acquisition requirements become cumbersome. In an active approach, a set of transducers interrogate the structure using pitch-catch monitoring in much the same way as the fatigue damage detection approach, described in the previous section. In the pitch-catch approach, damage is determined based on a change in the signals when compared to a baseline case.

A test specimen was constructed to simulate the skin components of the Bell 407 tail boom (Figure 13a). The length of the test specimen was 33 in. with a diameter of 15 in. and thickness of 0.04 in. An aluminum panel was rolled and mounted on a frame with bolts. One line of bolts was fixed to the side of the curved panel. The distance between each bolt was 1 in. which matches the distance between rivets used in the Bell 407 tail boom construction. The specimen was instrumented with in-situ piezoelectric transducers for interrogation during simulated ballistic event. A total of eight transducers were bonded to the structure (Figure 13b); four on each side with a spacing of 10 in. between the transducers and 4 in. from the bolt locations.

(a) tail boom skin section
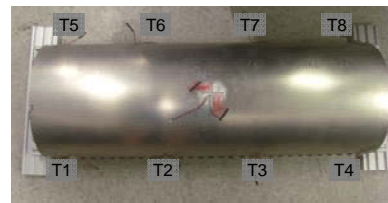
(b) transducer layout

Figure 13: Setup for tail boom skin damage detection

The actuation transducer was excited using a 5-cycle tone burst of 80 kHz. Data was acquired for pitch-catch cases where one transducer was set as an actuator and the remaining transducers were used as sensors. This was repeated until each transducer was used as an actuator. Damage index values were determined based on the difference between the responses for undamaged and damaged conditions. For damage detection, indices were categorized into three groups. One group corresponded to adjacent transducers. The damage index D_{12} corresponds to transducers T1 as the actuator and T2 and as the sensor. The second group corresponded to transducers located across width of the tail boom section. The damage

index D_{26} corresponds to transducers T2 and T6. The third group corresponded to transducers located diagonally across width of the tail boom section. The damage index D_{17} corresponds to transducers T1 and T7. Ballistic damage was artificially inserted near the T2 transducer approximately 4 in. laterally and 2 in. vertically, as shown in Figure 14.
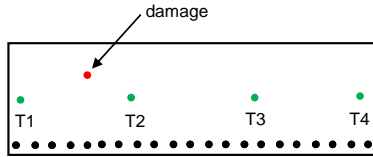

Figure 14: Position of ballistic damage

The damage index values are shown in Figure 15 for the case where the damage was approximately 0.3 in. in diameter. The results are categorized according to adjacent transducers along the length, transducers positioned directly across in the width direction, and transducers positioned diagonally. The damage indices used for detection correspond to transducer pairs T1 and T7 in the diagonal direction and transducer pairs T2 and T7 in the width direction (Figure 15b and c).
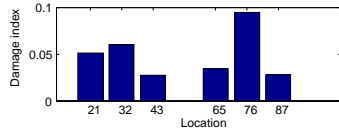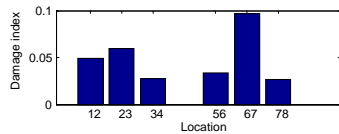
(a) transducers positioned adjacent
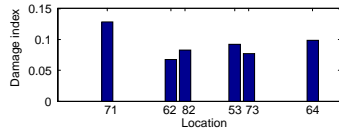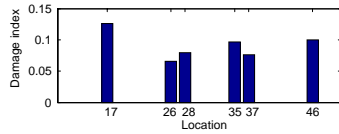
(b) transducers across width direction
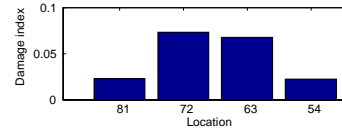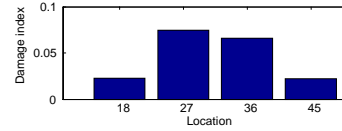
(c) transducers along diagonal directions

Figure 15: Damage indices corresponding to 0.3 in. diameter hole

The paths corresponding to these damage indices are shown in Figure 16. The general location of the damaged region was determined based on the evaluation of the damage indices and correlation with transducer layout. In this manner a set of distributed transducers form a network of paths which are able to identify an approximate the location of the damage. The results were similar when considering damage of various sizes. The average of the maximum damage indices in each direction was determined and plotted versus damage size (Figure 17). Additional testing is still required to validate the correlation between damage size and damage index.
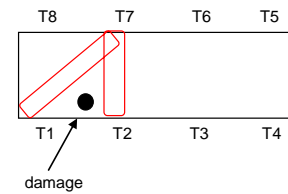

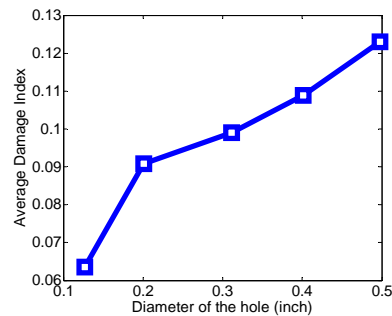Figure 16: Paths corresponding to largest damage indices in width and diagonal directions

Figure 17: Growth of damage index with damage size

Detection of Ballistic Battle Damage - Frame

Tail boom frame sections are roughly ring type structures installed at discrete locations along the span

of the structure (Figure 18). Frame structures are significantly more difficult to inspect than skins, so a sensor based damage detection approach was developed.
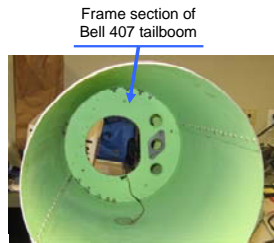

Figure 18: Frame section of tail boom

A Bell 407 tail boom representative frame section (Figure 19) was fabricated using 0.04 in. thick aluminum material. Piezoelectric transducers were mounted at the four quadrants of the specimen. Ballistic damage detection was conducted on the frame using a pitch-catch approach between adjacent transducers. The actuator and sensor assignments were rotated to interrogate the entire frame specimen. The actuation elements were excited using a tone burst signal of 5 cycles at 80 kHz to create the interrogation signal for the frame structure.
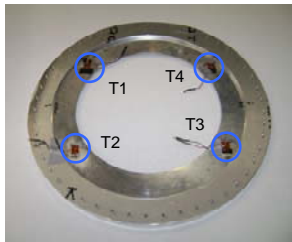

Figure 19: Specimen for frame section

A ballistic damage scenario was simulated by drilling a hole in the region between transducers T1 and T2. The damage index was constructed by comparing the transient response of the undamaged frame to the damaged. For the case where damage was a 0.155 in. diameter hole, the damage indices were tabulated and shown in Figure 20a. The damage index for the case where the damage size was increased to approximately 0.31 in. diameter is shown in Figure 20b.
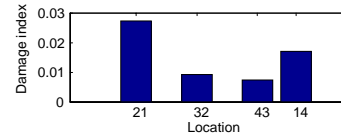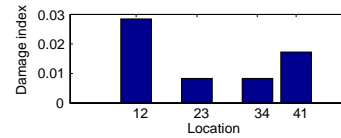
(a) 0.155 in. diameter hole
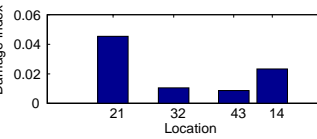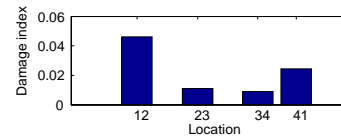
(b) 0.31 in. diameter hole

Figure 20: Damage indices corresponding to 0.155 in. diameter hole

The results showed that damage was able to be detected and the relative location determined, since the path between transducers T1 and T2 had the largest damage index. The location of damage was confirmed for the damage sizes ranging from 0.155 in. to 0.5 in. diameter. A plot of the average damage index for the T1-T2 path is shown in Figure 21. The damage index grows monotonically with the size of the damage. The damage index is an indicator of damage and its location, as well as an approximation of its size. Additional testing is required to verify these trends when repositioning the damage relative to the transducers.
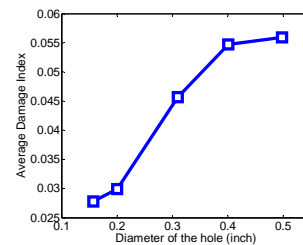

Figure 21: Growth of damage index with damage size

Effect of Temperature on Transducer

An experimental setup was used to determine the effect of temperature on the response of the piezoelectric elements. The experimental specimen with mounted transducers is shown in Figure 22a. The specimen was placed in a heating/cooling chamber as

shown in Figure 22b. Thermocouples were mounted to the specimen to get the material temperature. Data was gathered for temperatures ranging from –60°F to 200°F.
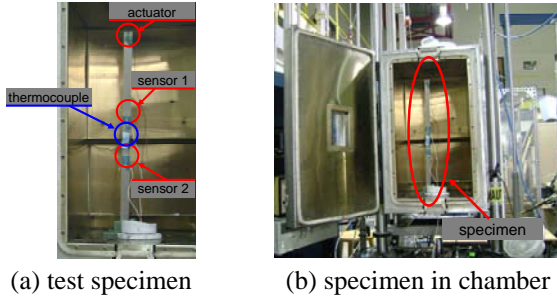

(a) test specimen   (b) specimen in chamber

Figure 22: Test setup to evaluate temperature effects

The recorded responses for sensors 1 and 2 at 80°F, 200°F, and -60°F for 80 kHz excitation is shown in Figure 23. It is apparent from the sensor signals that the amplitudes of the signals have shifted due to temperature.
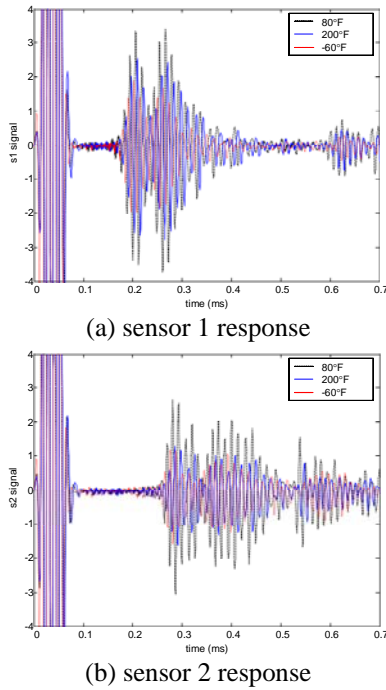

(a) sensor 1 response

(b) sensor 2 response

Figure 23: Sensor response for 80 kHz excitation (80°F, 200°F, and -60°F)

The signals were analyzed at each of the test conditions to determine the effect of temperature on the incident wave packet in terms of magnitude. The sensor signals were windowed in order to capture the incident waveform packet from the actuator location. The magnitude of the frequency component corresponding to the excitation frequency was determined using the following expression:

$$\phi = \frac{1}{T}\int_0^T s_w(t)\exp(i2\pi f_c t)\,dt$$

where $s_w(t)$ is the windowed sensor signal, f_c is the center frequency of the narrowband excitation signal. The magnitude of ϕ was normalized with respect to data taken at an 80°F reference value. The resulting expression was tabulated across the evaluated temperature ranges and excitation frequencies.
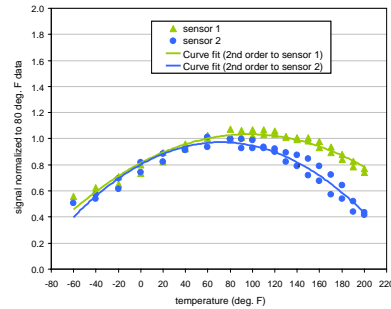

Figure 24: Normalized ϕ for 80 kHz excitation

Curve fits were performed for each of the normalized ϕ curves and the results for 80 kHz are shown in Figure 24. This process was repeated for all of the tested frequencies. The analysis resulted in the following temperature compensation equation:

$$\overline{\phi} = aT^2 + bT + c$$

where a, b, and c correspond to the curvature, slope, and offset of the curve. In the above relation, T is defined in terms of °F. For 80 kHz case, the values of a, b, c were determined to be -2.82E-05, 0.004646, and 0.808072, respectively.

The effect of temperature on the transducers and resulting damage index is understood and captured by the compensation equation.

System Design

A prototype system was designed to provide an on-board structural diagnostics capability. This system was tailored for an Acousto-Ultrasonic pitch-catch transducer network. The system consists of a data acquisition unit, excitation circuitry, microcontroller unit, multiplexer, thermocouple unit, and a communications subsystem that interfaces with a HUMS processor (Figure 25). The prototype system has the ability to perform additional data reduction functions with the addition of digital signal processors

to off-load the HUMS processor. This prototype system will be used in the technology demonstration on the Bell 407 tail boom. A small form factor unit has been designed to be used with 32 piezoelectric transducers. The unit has a designed footprint of approximately 36 sq. in. and a weight of approximately 3 lbs.
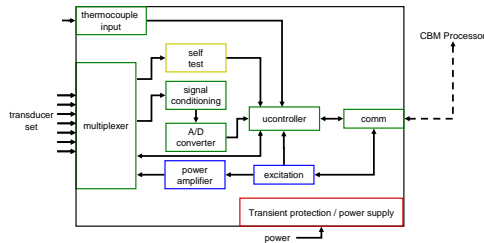

Figure 25: Conceptual design of testing system

Conclusions

This research has developed a technique using Acousto-Ultrasonics and in-situ piezoelectric transducers to detect fatigue crack and ballistic damage. Laboratory testing was conducted to demonstrate the feasibility and applicability of this technology for health monitoring of aerospace structures. Fatigue damage detection was demonstrated on coupon level testing for both crack open and crack closed cases. Sensor arrangements for fatigue hot spot locations and ballistic damage detection was identified and used to detect artificially inserted damage. Temperature testing was used to determine compensation techniques. A prototype on-board system design was identified.

This technology development serves as the foundation for the full scale technology demonstration on the Bell Model 407 tail boom, where both the fatigue and ballistic damage detection capability will be validated. As part of this effort, this technology will be integrated with other system diagnostic technologies into a common HUMS with the goal of providing confidence in transitioning the Structural Health Monitoring to civilian and military aircraft.

References

1. Hunt, S.R. and I.G. Hebden, *Validation of the Eurofighter Typhoon structural health and usage monitoring system.* Smart Materials and Structures, 2001. **10**(3): p. 497-503.
2. Monnier, T., *Lamb Waves-based Impact Damage Monitoring of a Stiffened Aircraft Panel using Piezoelectric Transducers.* Journal of Intelligent Material Systems and Structures, 2006. **17**(5): p. 411-421.
3. Zhao, X., et al., *Active health monitoring of an aircraft wing with embedded piezoelectric sensor/actuator network: I. Defect detection, localization and growth monitoring.* Smart Materials and Structures, 2007. **16**(4): p. 1208-1217.
4. Jackson, K.J., et al., *Structural Condition Monitoring of Royal Australian Air Force F-111 and F/A-18 Aircraft*, in *6th Joint FAA/DOD/NASA Aging Aircraft Conference*. 2002: San Fransisco, CA.
5. Caron, Y. and Y. Richard, *CF-188 Fatigue Life Management Program*, in *RTO AVT Specialists Meeting on Exploitation of Structural Loads/Health Data for Reduced Life Cycle Costs*. 1998: Brussels, Belgium.
6. Land, J.E., *HUMS - The Benefits - Past, Present, and Future*, in *IEEE Proceedings: Aerospace Conference*. 2001: Big Sky, MT. p. 3083-3094.
7. Cawley, P. and D. Alleyne, *The use of Lamb waves for the long range inspection of large structures.* Ultrasonics, 1996. **34**(2-5): p. 287-290.
8. Purekar, A.S., et al., *Directional piezoelectric phased array filters for detecting damage in isotropic plates.* Smart Materials and Structures, 2004. **13**(4): p. 838-850.
9. Gentzen, V., et al. *Experimental detection and quantitative interrogation of damage in a jointed composite structure*. in *Smart Materials, Adaptive Structures, and Intelligent Systems*. 2008. Ellicott City, Maryland: ASME.
10. Choi, Y.-T., A.S. Purekar, and N.M. Wereley. *Torque loss and crack monitoring near fasteners for isotropic and composite helicopter tail boom structural models*. in *Smart Materials, Adaptive Structures, and Intelligent Systems*. 2008. Ellicott City, Maryland: ASME.
11. Yoo, B., A.S. Purekar, and D.J. Pines. *Guided lamb wave interrogation of a curved composite plate [0/90] using the Hilbert-Huang Transform approach*. in *Smart Materials, Adaptive Structures, and Intelligent Systems*. 2008. Ellicott City, Maryland: ASME.
12. Purekar, A.S., *Piezoelectric Phased Array Acousto-Ultrasonic Interrogation of Damage in Thin Plates*, in *Aerospace Engineering*. 2006, University of Maryland: College Park.
13. Galan, J.M. and R. Abascal, *Numerical simulation of Lamb wave scattering in semi-infinite plates.* International Journal for Numerical Methods in Engineering, 2002. **53**(5): p. 1145-1173.